第 48 卷 第 7 期
2021 年 7 月

湖南大学学报（自然科学版）
Journal of Hunan University（Natural Sciences）

Vol. 48. No. 7.
July 2021

Open Access Article

Clustering-Based Quantitative Evaluation Using Acoustic Emission Waveforms for Corrosion Detection

Farrukh Hassan[1*], Ahmad Kamil Mahmood[1], Lukman Ab. Rahim[1], Syed Muslim Jameel[2], Abdul Saboor[1], Mohamed Rimsan[1]

[1] High Performance Cloud Computing Centre (HPC3), Department of Computer & Information Science, Universiti Teknologi PETRONAS, Seri Iskandar, Perak, Malaysia

[2] Department of Software Engineering, Sir Syed University of Engineering and Technology, Karachi, Pakistan

Abstract: Acoustic emission technique has been used commonly now a day for mechanical diagnostics. These events need to be discriminated against due to various kinds of damages in composite materials. Continuous wavelets transform (CWT) has been used to generate scalograms. Structural similarity index measure (SSIM) generates the similarity index table of these scalograms. The performance of various clustering techniques, such as k-means, k-medoids, the Hierarchical clustering was evaluated by several validity indices such as Dunn's Index, Davies Bouldin Index, Silhouette Index, Calinski-Harabasz index, and the execution time. We use acoustic emission data to verify the application of these techniques. The results demonstrated that the execution time of the k-means clustering is the shortest, and silhouette, Davies Bouldin, and Calinski-Harabasz give the best possible value for (K=2).

Keywords: continuous wavelet transform, structural similarity index, acoustic emission, clustering techniques, cluster validation indices.

使用聲發射波形進行腐蝕檢測的基於聚類的定量評估

摘要：

聲發射技術現在已普遍用於機械診斷。由於復合材料中的各種損壞，這些事件需要加以區分。連續小波變換(CWT)已被用於生成標量圖。結構相似性指數度量(SSIM)生成這些尺度圖的相似性指數表。各種聚類技術（例如k均值、克-
中心點、分層聚類）的性能通過多個有效性指標（例如鄧恩指數、戴維斯博爾丹指數、剪影索引、卡林斯基· 哈拉巴斯,指標和執行時間）進行評估。我們使用聲發射數據來驗證這些技術的應用。結果表明，均值聚類的執行時間最短，而剪影、戴维斯· 博尔丹和卡林斯基· 哈拉巴斯給出了(钾=2) 的最佳可能值。

关键词： 膜、壓力驅動、非熱、滲透、滯留、海洋資源。

1. Introduction

Pipelines as the primary means for transporting oil and gas products play an essential role in upgrading a country's economy. With the current industrial advancement, the safety of these pipelines has become a significant concern. Damages develop in these pipelines gradually due to rough operational and environmental conditions, leading to severe safety accidents and

Received: April 18, 2021 / Revised: May 20, 2021 / Accepted: June 25, 2021 / Published: July 31, 2021

About the authors: Farrukh Hassan, Ahmad Kamil Mahmood, Lukman Ab. Rahim, High Performance Cloud Computing Centre (HPC3), Department of Computer & Information Science, Universiti Teknologi PETRONAS, Seri Iskandar, Malaysia; Syed Muslim Jameel, Department of Software Engineering, Sir Syed University of Engineering and Technology, Karachi, Pakistan; Abdul Saboor, Mohamed Rimsan, High Performance Cloud Computing Centre (HPC3), Department of Computer & Information Science, Universiti Teknologi PETRONAS, Seri Iskandar, Malaysia

pollution. The corrosion in steel pipelines, which occurs due to chloride attack and carbonation phenomena, can reduce its lifetime significantly [1]. Commonly used techniques for identifying corrosion damages include magnetic flux leakage tests, acoustic emission (AE), eddy current tests, and ultrasonic tests. Among which AE has been widely used during recent years.

Acoustic Emission (AE) is produced in transient elastic sound waves due to the release of localized stress-energy when any deformation occurs in a material. AE is commonly observed in the 50 kHz to 1 MHz frequency range. The AE approach can identify a wide range of growing defects, but during the last two decades, localized corrosion processes have gained significant attention [2], [3], [4]. AE signals provide valuable information about the damage mechanisms. The discrimination of these signals produced from various damages is a significant challenge of AE analysis [5].

Generally accepted ways of discriminating AE signals can be divided as supervised and unsupervised. Supervised learning has been used, which relies on labeled data. The quantity and quality of labeled training data are crucial for determining the effectiveness of an algorithm. Morizet et al. [6] introduced a classification approach for localized corrosion to simulate different degrees of uncertainties on labeled data. The exact knowledge about AE sources is not possible, which results in the unavailability of the training data belonging to specific damages. The clusters are labeled, in such a case, by cluster analysis. Wu et al. [7]. Compared the performance of acoustic emission (AE) monitoring and three-dimensional (3D) X-ray computed tomography (XCT) scanning for localized corrosion and cracking. Zhang et al. [8] discussed the relationship between the AE waveform and SCC(Stress Corrosion Cracking) process. Calabrese et al. [9] monitored the AE activity as the progression of various corrosion damages in large-scale pre-stressed concrete beams. Similarly, Velez et al. could detect the corrosion activity in large-scale portions of pre-stressed concrete piles placed in seawater. [10]. Abouhussien and Hassan could validate the application of the acoustic emission (AE) technique for assessing localized reinforcement corrosion damages in large-scale RC beams [11]. However, there is no literature on identifying corrosion damage in long-range steel pipelines using the AE approach.

This paper presents an approach to applying acoustic emission technology to detect artificially created corrosion damage in steel pipelines. Based on the findings, this work presents a data-driven AE monitoring technique that combines wavelet scalograms with the SSIM approach to determine the state and remaining useful life of a pipeline. The individual hits were transformed into scalograms by using CWT. The SSIM table is generated by comparing each scalogram to the rest of the scalograms. The clustering performance of various algorithms such as k-means, hierarchal, k-medoids is validated by multiple clusters validation indices such as the silhouette, Davies Bouldin, Dunn's index, and Calinski-Harabasz.

The organization of the rest of the article is as follows: The introduction section gives an overview of corrosion monitoring using acoustic emission. The related work section provides the literature about the unsupervised clustering used in AE data. The "Methodology" section presents our model design, dataset description, and methods. The outcomes of the proposed method are discussed in the "Results and discussion" section. The "Conclusion" section concludes the article.

2. Literature Review

The promising outcomes of the recent research [6], [12], [13], [14] indicate that machine-learning algorithms will be a powerful alternative to the currently available algorithms for the processing of acoustic emission data. However, supervised learning has been used rarely because the quantity and quality of labeled training data are crucial for determining an algorithm's effectiveness. The unavailability of training data urges the use of an unsupervised approach for grouping AE data.

Several authors attempted to optimize the classification accuracy of AE data. To improve the accuracy and reliability of the pattern recognition approaches, Pappas et al. [15] proposed an algorithm for analyzing AE data. The clustering procedure produced promising results which were significantly correlated to the active damages mechanisms. Shahidan et al. [16] successfully detected various damage processes by implementing k-means and a NN. NN achieved an accuracy rate of 99%. Johnson [17] used PCA as an unsupervised method to cluster the AE data collected during tensile testing on glass fiber/epoxy laminates. AE signals from various matrix cracking and local delamination clusters were efficiently separated. SOM and k-means algorithms were used by Gaertner and Godin [17] to detect the AE signals collected during tensile testing on cross-ply glass/epoxy composites. When unsupervised clustering was applied to AE signals, three clusters were obtained. A cumulative plot of the events described the formation and evolution of each failure mechanism. Bar et al. [19] investigated the noisy AE signals. The data was acquired with PVDF sensors to identify the matrix and fiber failures. He used ANN for the classification of AE signals having highly overlapping parameters. De Oliveira and Marques

[20]classified the AE data using unsupervised pattern recognition algorithms based on an artificial neural network. Time-scale diagrams belonging to specific clusters were obtained. During the tensile testing of cross-ply glass fiber/polyester laminates, six distinct AE waveforms were captured. Philippidis et al. [21] conducted similar research by using ANS techniques for clustering similar AE signals emitted from 2D woven C/C laminates. Fractographic data from the damaged tensile coupons confirmed the identification of various damages. Huguet et al. [22] employed a statistical method called a Kohonen neural network to identify similar signals successfully. Chandrashekhar et al. [23] obtained the AE signals from fatigue spectrum load testing on CFRP specimens were investigated. The noise was removed by combining supervised and unsupervised techniques, and AE signals were then classified using a neural network. Karanth [24] investigated the FCM clustering approach and ACO approaches to categorize AE signals by their separate sources. Because both ANN and FCM can handle calls with many overlapping features, no prior knowledge of data distribution is necessary. Behnia et al. [25] employed the principal component technique and unsupervised kernel fuzzy c-means analysis to identify different phases of deterioration in plain and steel fiber reinforced concrete specimens monitored using the AE technique.

The deep neural network has brought a revolution in feature extraction, data denoising, and big data classification. To address the human error issue in traditional AE technology, an image-based deep learning solution was presented by Ebrahimkhanlou and Salvatore [26] for the localization of cracks in plate-like structures. Suwansin and Pattarapong [27] proposed a deep learning algorithmic model to detect cracks in the steel rail. The overall accuracy was 77.33% under the onsite experiment. A stacked AE is a deep neural network made up of numerous AEs. The depth of SAE can easily be increased to accommodate complex data and reflect nonlinear features adequately. Wang et al. [28] suggested extracting damage-related features in mechanical systems implying GG clustering. It could successfully split the damage phase of the machinery. GG clustering has several drawbacks including, (a) identifying the ideal number clusters is tricky (b) It ignores the impact of diverse data types on the clustering process. (c) if the initial cluster centers are not adequately chosen, it is quite possible to fall into the local optimum solution. Analyzing vast volumes of unlabeled data is a tedious and intensive task. To overcome this issue, Hu et al. [29] integrated SSAE into AWGG clustering to propose DAFC for the clustering analysis of big industrial data. The DAFC model takes less time than its competing models, such as SAE+FCM, SSAE+GK, and SSAE+GG, implying that the AWGG clustering is more effective.

3. Methods/Materials

The recorded AE signals are the transient waves that a waveform reflects. The frequency information of a signal cannot be extracted in time domain representation. Only stationary and periodic signals are included in a frequency-based analysis. Frequency analysis is not capable of retrieving the time-related data of a signal [30]. According to [31], the essential features of the AE signals vary in duration and frequency. Therefore time-frequency analysis is seen to be a desirable method for extracting more significant AE characteristics. The time in-variant nature of the frequency components may be evaluated using time-frequency analysis.

3.1. Continuous Wavelet Transform

The summation of the signal throughout all time multiplied by scaled, shifted variants of the wavelet function is the continuous wavelet transform [32]. CWT has been used successfully to identify the hidden secrets and short-time events, recognize the patterns, extract multi-resolution features, and compress data.

We require a mother wavelet ∈ L2 to implement CWT, limiting the duration and zero average. According to [32], To qualify, the following conditions must be met by the mother wavelet ψ(t): The function integrates to 0 as

$$\int_{-\infty}^{\infty} \psi(t)dt = 0 \qquad (1)$$

The acceptability requirement is satisfied by its Fourier transform ψ(ω) as

$$CWT_{(a,b)} = \int_{-\infty}^{\infty} \frac{|\psi(\omega)|^2}{\omega} d(\omega) < \infty \qquad (2)$$

After selecting the mother wavelet, Eq. 3 defines the CWT of the function $f(t) \in L2\ (\mathbb{R})$.

$$CWT_{(a,b)} = (f, \psi\ a, b) = \frac{1}{\sqrt{a}} \int_{-\infty}^{\infty} f(t)\, \psi * \left(\frac{t-b}{a}\right) \mathrm{dt}, \qquad (3)$$

To analyze the AE data acquired in our experimental setup, the morlet wavelet is employed as the mother wavelet. According to [28], the morlet wavelet is the optimal balance between temporal and frequency resolution. It is commonly used for detecting and identifying confidential information in transient events.

3.2. Structural Similarity Index Measure (SSIM)

The SSIM method evaluates the degree of similarity between two images, classifying the damage type and identifying its location. The comparison function of

luminance, contrast, and the structure of two images x is given by Eq. 4, 5, and 6.

$$l(x,y) = \frac{2\gamma_x\gamma_y + R_1}{\gamma_x^2 + \gamma_y^2 + R_1} \quad (4)$$

$$c(x,y) = \frac{2\vartheta_x\vartheta_y + R_2}{\vartheta_x^2 + \vartheta_y^2 + R_2} \quad (5)$$

$$s(x,y) = \frac{\vartheta_{xy} + R_3}{\vartheta_x\vartheta_y + R_3} \quad (6)$$

where γ_x and γ_y, ϑ_x and ϑ_y, and ϑ_{xy} are the local means, standard deviations, and cross-covariance of image x and image y, respectively, the regularization constants R_1, R_2, and R_3 possess tiny values to neglect the extreme small denominator. By merging the three sub-functions, the equation for SSIM index can be represented as Eq. 7:

$$SSIM(x,y) = \frac{(2\gamma_x\gamma_y + R_1)(2\vartheta_{xy} + R_2)}{(\gamma_x^2 + \gamma_y^2 + R_1)(\vartheta_x^2 + \vartheta_y^2 + R_2)} \quad (7)$$

The result of the SSIM equation is equal to 1 only when an image is compared to itself. An index value lower than 1 shows the degree of dissimilarity between two images. The mean of the index map is equal to the sum of SSIM and the sub-indices of the compared images. The methodology has been depicted in Algorithm(1) and Figure 3.

3.3. Experimental Setup

Two sets of 4 sensors (R6I) were mounted on a steel pipeline (7.625 m) apart from one another, as shown in Figure 1. Defects were fabricated on the surface of a pipe by employing Reverse Impressed Current Cathodic Protection (RICCP) technique at a distance (1.04 m) from set 2. The data acquisition system includes integrated amplifier AE sensors (R6I), Physical acoustic manufactured Express-8 PCI express based 16 – channel AE system, and AEwin software. The threshold value of AE is set to 35 dB, and the sampling rate is 1 MHz, and the working frequency range is 35–100 kHz.

3.4. Dataset

The AE data were continuously collected for one hour. The total number of hits recorded by the system for the entire duration was 171. Each hit is represented by one waveform and is composed of 2048 data points obtained in 0.002048 sec. The CSV file contains information about each impact as a single ".csv file." All these separate CSV files are then combined into a single .csv for individual sensors. Sensor-1 received 65 hits, the highest, and sensor 5 and 8 the least number of hits 7. Figure 2 shows the histogram of the similarity index values, which capture the outliers that do not satisfy $|X| < 4$.

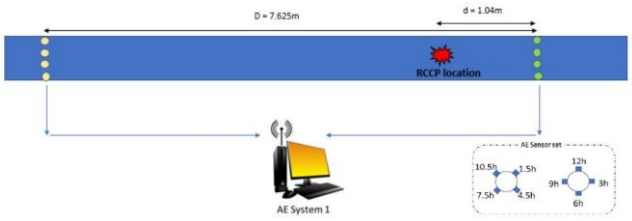

Fig. 1 Experimental setup for data acquisition

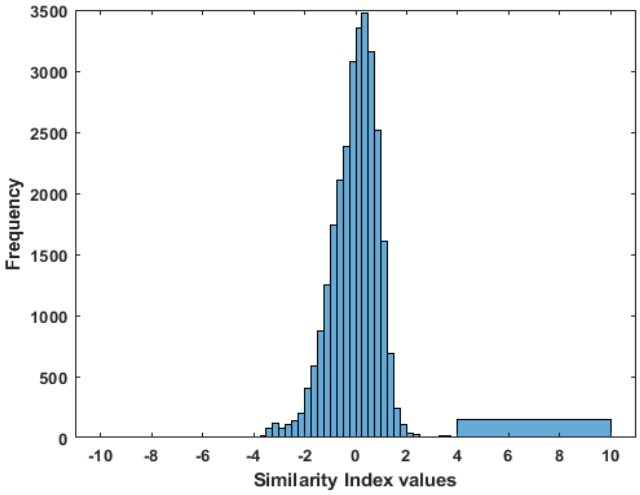

Fig. 2 Histogram of the dataset

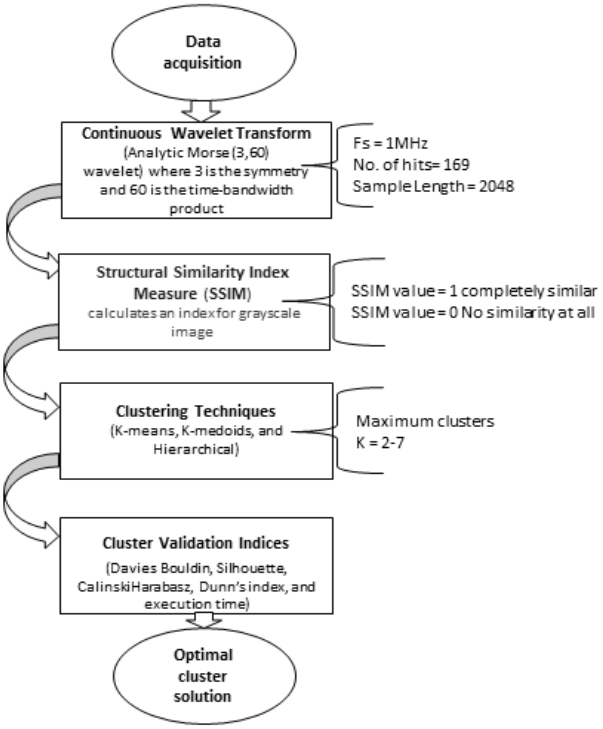

Fig. 3 Main flow chart of the program used in this study

Algorithm (1): AECLUSVAL
Input data:

- AE hits are separated channel wise.
- Each hit is transformed into a scalogram using CWT.
- For i = sgm_{min} to sgm_{max}
- For j = sgmmin to sgmmax

- Calculate SSIM(i,j)
- j = j +1
- End
- i = i+1
- End
- For k = 2 to 7
- Perform Kmeans, K-medoids, and hierarchical clustering
- Calculate the validation indices
- End

Select the optimal value of k.

4. Results and Discussion

External, relative, and external are the three ways by which the clusters may be validated. Adjusted Rand Index is an external measure that aims to compare the clustering results to a ground truth solution. Since clustering is an unsupervised approach, external actions are not applicable in practice. Internal and relative validity approaches are desirable for real-world applications. Internal criteria are used to assess the quality of a clustering solution based only on the data. Relative criteria are internal criteria that can evaluate two clustering structures and determine the superior one in terms of comparable value [33]. The performance results of various validation indices three clustering algorithms have been presented in Table 1.

4.1. Silhouette Index Evaluation

For k-means, hierarchical, and k-medoids clustering, the Silhouette validity graph is shown in Fig. 4. The range of the Silhouette values is from -1 to 1. A number closer to 1 denotes that the data point has been assigned to a suitable cluster. A value close to zero can be allocated to another collection because it lies at an equal distance from both groups. The importance of misclassified data and lie somewhere close to –1. The generated silhouette values in the results reveal that all the techniques generate values between 0 and 1. The generated values clustering algorithms are maximum at k=2. With an increase in k, silhouette value slightly decreases.

4.2. Davies Bouldin Index Evaluation

Fork-means, hierarchical, and k-medoids clustering, the Davies Bouldin (DB) validity graph is shown in Figure5 concerning the number of clusters k. This index aims to reduce the average intra-clusters distance as much as possible. From the chart, the values of this index for the three clustering algorithms increases gradually. Hierarchical clustering outperforms the other techniques with a high DB index value of 1.6620.

4.3. Evaluation Using Calinski-Harabasz Index

Figure 6 shows the Calinski-Harabasz index values as a function of the number of clusters k. This index is a kind of estimate that chooses the correct clustering number before performing the algorithm. From the graph, K-medoids clustering outperforms k-means and hierarchical clustering for k=2. The performance of all the algorithms decreases gradually with an increase in the number of clusters k.

4.4. Evaluation Using Dunn's Index

Figure 7 displays the Dunn's validity index graph for various clusters k. The measure aims to increase the distance between multiple clusters while decreasing the distance between the data points within the same cluster. In the case of Dunn's validity measure, the graph displays that k-means clustering excels.

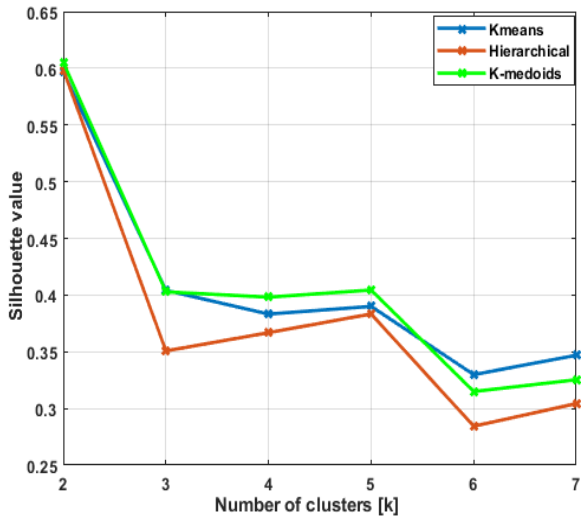

Fig. 4 The impact of several clusters on the Silhouette Validity Index

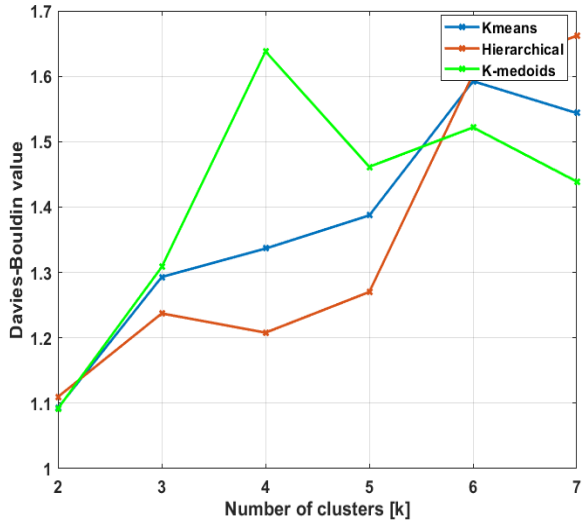

Fig. 5 The impact of several clusters on the Davies Bouldin Index

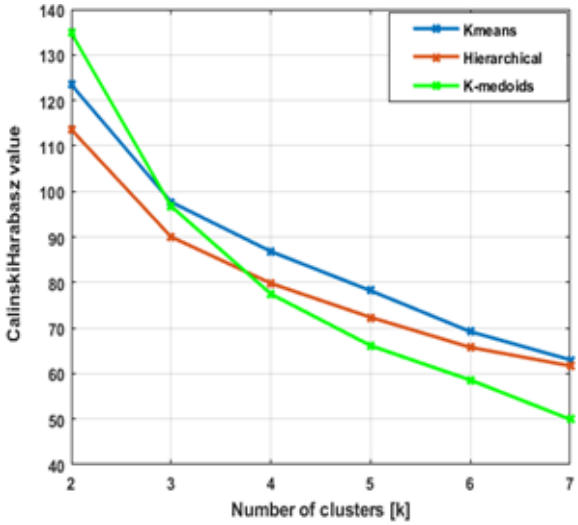

Fig. 6 The impact of several clusters on Calinski-Harabasz Validity Index

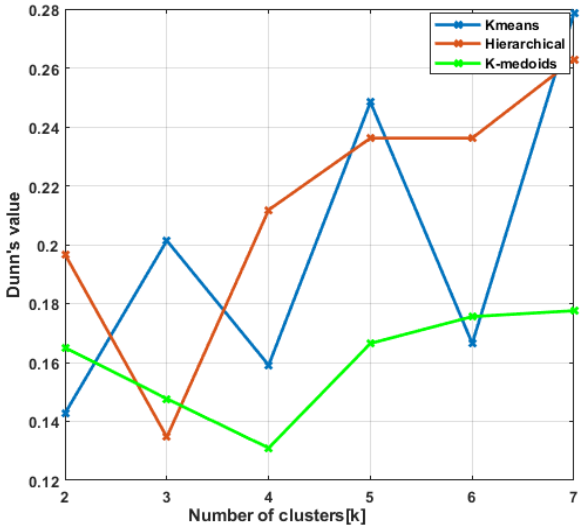

Fig. 7 The impact of several clusters on Dunn's Validity Index

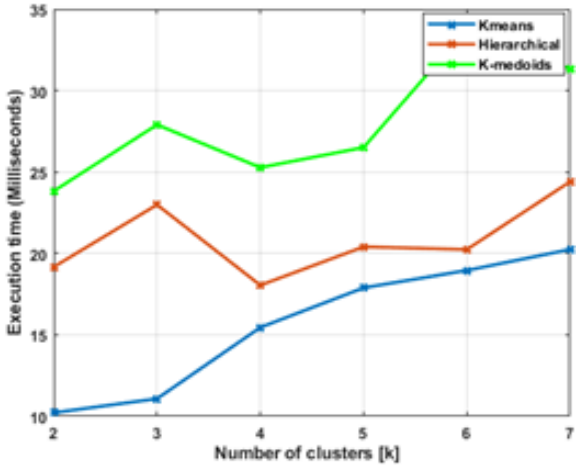

Fig. 8 The impact of several clusters on execution time

Table 1 Performance evaluation of K-means, K-medoids, and hierarchical clustering

	No. of Clusters	Dunn's	Silhouette	Davies Bouldin	Calinski-Harabasz	Execution Time
K-means	02	0.1428	0.5969	1.0931	123.4559	10.224
	03	0.2014	0.4042	1.2932	97.6919	11.085
	04	0.1591	0.3833	1.3366	86.8167	15.461
	05	0.2484	0.3901	1.3873	78.2052	17.892
	06	0.1665	0.3299	1.5925	69.2104	18.962
	07	0.2787	0.3470	1.5437	63.0213	20.250
Hierarchical	02	0.1967	0.5985	1.1099	113.5783	19.177
	03	0.1347	0.3508	1.2374	90.0361	22.994
	04	0.2118	0.3669	1.2080	79.8212	18.051
	05	0.2362	0.3834	1.2702	72.3528	20.412
	06	0.2362	0.2844	1.6030	65.7568	20.247
	07	0.2629z	0.3044	1.6620	61.7086	24.409
K-Medoids	02	0.1430	0.6052	1.0920	134.7852	23.834
	03	0.1089	0.4029	1.3085	96.7735	27.907
	04	0.1108	0.3982	1.6380	77.4949	25.278
	05	0.1756	0.4045	1.4617	66.1317	26.510
	06	0.1756	0.3150	1.5218	58.5785	33.786
	07	0.1776	0.3254	1.4390	49.9498	31.342

4.5. Evaluation of Time Performance

Figure 8 displays the time taken by each clustering technique to execute in milliseconds with an increase in the number of clusters k. Our findings suggest that *k* means clustering algorithm is the fastest when the k=2 with an execution time of 10.2240. K-medoids clustering

(with k=5) is the slowest, with an execution time of 33.7860.

The identification of acoustic emission signals might be challenging because of the pervasive noise in the operating conditions in practical applications. Acoustic emission signals have been used to detect corrosion initiation in a variety of materials. However, the behavior of the movement is constrained by the nature and shape of the specimens, as well as the type of AE sensors used.

5. Conclusion

Cluster analysis seeks to uncover the intrinsic characteristics of the concerned data set. It assesses the clustering results and chooses the optimal scheme. Most of the algorithms specify how many clusters a data set should be divided. The actual number of clusters needs to be validated because clustering is an unsupervised method.

This paper presented a detailed overview of various clustering techniques for acoustic emission data. Several indices such as Dunn's index, Silhouette index, Davies-Bouldin index, Calinski-Harabasz index, and execution time were discussed to evaluate the validity of clusters. The execution times of various algorithms are recorded and used to assess time performance.

- For the ideal number of K=2, K-medoids clustering delivers the highest accuracy in terms of silhouette validity index. The hierarchical method has higher accuracy than the k-means algorithm.
- Dunn's index measures the distances between different clusters and the distance between the data points within the same cluster. In terms of Dunn's index, the k-means algorithm outperforms the k-medoids and hierarchical clustering for K=2. With an increase in the number of clusters, a variation is seen in this index value. For K=7, k means clustering gives the worst performance.
- Our findings suggest that k-means clustering method has the best time performance and gradually improves with time as the number of clusters K increases. Hierarchical clustering algorithm gives reasonably better time performance than the k-medoids algorithm. K-medoids takes much more execution time than all other algorithms, and thus it has the most deficient performance in terms of time.

A quality validation metric can accurately assess the quality of these clusters, including the intra-cluster quality, inter-cluster separation, and the clusters' shape. Instead of employing a single representative point, a group of representative points or multidimensional curves can be used. One of the challenges is to develop an integrated quality evaluation approach for data mining findings. It will significantly contribute to data mining approaches for finding exciting and valuable patterns in the acoustic emission data.

Nomenclatures	
Symbols	
μ_x, $\mu_y\sigma_x$,	The local mean of images X and Y
σ_y	Standard derivation of image X and Y
σ_{xy}	Cross-covariance
C1, C2, C3	Regularization constants
ψ(t)	Mother wavelet
Abbreviations	
AE	Acoustic Emission
SSIM	Structural Similarity Index Measure
CWT	Continuous Wavelet Transform
WHO	World Health Organization
RICCP	Reverse Impressed Current Cathodic
PVDF	Polyvinylidene fluoride
SOM	Self-Organizing Map
PCA	Principle Component Analysis
ACO	Ant Colony Optimization
FCM	Fuzzy C-Means
NN	Neural Network
ANN	Artificial Neural Network
ANS	Artificial Neural System
DAFC	Deep Adaptive Fuzzy Clustering Algorithm
SSAE	Stacked Sparse Autoencoder
AWGG	Adaptive Weighted Gath-Geva
GG	Gath-Geva

References

[1] HREN M., BOSILJKOV B. V., and LEGAT A. Effects of blended cement and carbonation on chloride-induced corrosion propagation. *Cement and Concrete Research*, 2021, 145: 106458. https://doi.org/10.1016/j.cemconres.2021.106458

[2] MANGALGIRI P. D. Corrosion issues in structural health monitoring of aircraft. *ISSS Journal of Micro and Smart Systems*, 2019, 8(1): 49–78. https://doi.org/10.1007/s41683-019-00035-z

[3] KARVELIS P., GEORGOULAS G., KAPPATOS V., and STYLIOS C. Deep machine learning for structural health monitoring on ship hulls using acoustic emission method. *Ships and Offshore Structures*, 2020, 16(1): 1–9. https://doi.org/10.1080/17445302.2020.1735844

[4] GOLDARAN R., TURER A., and OZLUTAS K. Identification of corrosion in a pre-stressed concrete pipe utilizing acoustic emission technique. *Construction and Building Materials*, 2020, 242: 118053. https://doi.org/10.1016/j.conbuildmat.2020.118053

[5] CALABRESE L., GALEANO M., PROVERBIO E., DI PIETRO D., CAPPUCCINI F., and DONATO A. Monitoring of 13% Cr martensitic stainless steel corrosion in chloride solution in presence of thiosulphate by acoustic emission technique. *Corrosion Science*, 2016, 111: 151–161. https://doi.org/10.1016/j.corsci.2016.05.010

[6] MORIZET N., GODIN N., TANG J., MAILLET E., FREGONESE M., and NORMAND B. Classification of acoustic emission signals using wavelets and random forests: Application to localized corrosion. *Mechanical Systems and Signal Processing*, 2016, 70–71: 1026–1037. https://doi.org/ 10.1016/j.ymssp.2015.09.025

[7] WU K., ITO K., SHINOZAKI I., CHIVAVIBUL P., and ENOKI M. A comparative study of localized corrosion and stress corrosion cracking of 13Cr martensitic stainless steel using acoustic emission and X-ray computed tomography. *Materials (Basel)*, 2019, 12(16): 1–19. https://doi.org/10.3390/ma12162569

[8] ZHANG Z., WU X., and TAN J. In-situ monitoring of stress corrosion cracking of 304 stainless steel in high-temperature water by analyzing acoustic emission waveform. *Corrosion Science*, 2019, 146: 90–98. https://doi.org/10.1016/j.corsci.2018.10.022

[9] CALABRESE L., CAMPANELLA G., and PROVERBIO E. Identification of corrosion mechanisms by univariate and multivariate statistical analysis during long-term acoustic emission monitoring on a pre-stressed concrete beam. *Corrosion Science*, 2013, 73: 161–171. https://doi.org/10.1016/j.corsci.2013.03.032

[10] ZIEHL M., MATTA F., VELEZ W. Acoustic emission monitoring of premature corrosion in pre-stressed concrete piles. *Structural Control and Health Monitoring*, 2014, 22(5): 873–887. https://doi.org/10.1002/stc.1723

[11] ABOUHUSSIEN A. A. and HASSAN A. A. A. Acoustic emission monitoring of corrosion damage propagation in large-scale reinforced concrete beams. *Journal of Performance of Constructed Facilities*, 32(2): 04017133. https://doi.org/ 10.1061/(ASCE)CF.1943-5509.0001127

[12] DAS A. K., SUTHAR D., and LEUNG C. K. Y.. Machine learning-based crack mode classification from unlabeled acoustic emission waveform features. *Cement and Concrete Research*, 2019, 121: 42–57. https://doi.org/10.1016/j.cemconres.2019.03.001

[13] HESSER D. F., MOSTAFAVI S., KOCUR G. K., and MARKERT B. Neurocomputing identification of acoustic emission sources for structural health monitoring applications based on convolutional neural networks and deep transfer learning. *Neurocomputing*, 2021, 453: 1–12. https://doi.org/10.1016/j.neucom.2021.04.108

[14] SHEIKH M. F., KAMAL K., RAFIQUE F., SABIR S., ZAHEER H., and KHAN K. Corrosion detection and severity level prediction using acoustic emission and machine learning-based approach. *Ain Shams Engineering Journal*, May 2021, in press. https://doi.org/10.1016/j.asej.2021.03.024

[15] PAPPAS Y. Z., MARKOPOULOS Y. P., and KOSTOPOULOS V. Failure mechanisms analysis of 2D carbon/carbon using acoustic emission monitoring. *NDT E International*, 1998, 31(3): 157–163. https://doi.org/10.1016/S0963-8695(98)00002-4

[16] SHAHIDAN S., PULLIN R., HOLFORD K. M., MUHAMAD B. N., and NOR N. Quantitative evaluation of the relationship between tensile crack and shear movement in concrete beams. *Advanced Materials Research*, 2013, 626: 355–359. https://doi.org/10.4028/www.scientific.net/AMR.626.355

[17] JOHNSON M. Waveform-based clustering and classification of AE transients in composite laminates using principal component analysis *NDT E International*, 2002, 35(6): 367–376. https://doi.org/10.1016/S0963-8695(02)00004-X

[18] GAERTNER S. H. R., GODIN N. Integration of Kohonen's self-organizing map and k-means algorithm to segmentation the AE data collected during tensile tests on cross-ply composites. *NDT E International*, 2005, 38(4): 299–309. https://doi.org/ 10.1016/j.ndteint.2004.09.006

[19] BAR H. N., BHAT M. R., and MURTHY C. R. L. Identification of failure modes in GFRP using PVDF sensors: ANN approach. *Composite Structures*, 2004, 65(2): 231–237. https://doi.org/ 10.1016/j.compstruct.2003.10.019

[20] MARQUES A. T., DE OLIVEIRA R. Health monitoring of FRP using acoustic emission and artificial neural networks. *Computers and Structures*, 2007, 86(3): 367–373. https://doi.org/10.1016/j.compstruc.2007.02.015

[21] PHILIPPIDIS T.P., NIKOLAIDIS V.N., ANASTASSOPOULOS A. Damage characterization of carbon/ carbon laminates using neural network techniques on AE signals. *NDT&E International*, 1998, 31(5): 329–340. https://doi.org/ 10.1016/S0963-8695(98)00015-2

[22] HUGUET S., GODIN N., GAERTNER R., SALMON L., and VILLARD D. Use acoustic emission to identify damage modes in glass fiber reinforced polyester. *Composites Science and Technology*, 2002, 62(10–11): 1433–1444. https://doi.org/ 10.1016/S0266-3538(02)00087-8

[23] BHAT C., BHAT M. R., and MURTHY C. R. L. Acoustic emission characterization of failure modes in composites with ANN. *Composite Structures*, 2003, 61(3): 213–220. https://doi.org/ 10.1016/S0263-8223(03)00068-0

[24] OMKAR S.N., RAGHAVENDRA KARANTH U. Rule extraction for the classification of acoustic emission signals using Ant Colony Optimisation. *Engineering Applications of Artificial Intelligence*, 2008, 21(8): 1381-1388. https://doi.org/10.1016/j.engappai.2008.02.004

[25] BEHNIA A., CHAI H. K., GHASEMIGOL M., SEPEHRINEZHAD A., and MOUSA A. A. Advanced damage detection technique by integration of unsupervised clustering into acoustic emission. *Engineering Fracture Mechanics*, 2019, 210: 212–227. https://doi.org/ 10.1016/j.engfracmech.2018.07.005

[26] EBRAHIMKHANLOU A. and SALAMONE S. Single-sensor acoustic emission source localization in plate-like structures using deep learning. *Aerospace*, 2018, 5(2): 1–22. https://doi.org/ 10.3390/aerospace5020050.

[27] SUWANSIN W. and PHASUKKIT P. Deep learning-based acoustic emission scheme for nondestructive localization of cracks in train rails under a load. *Sensors (Switzerland)*, 2021, 21(1): 1–19. https://doi.org/ 10.3390/s21010272

[28] WANG B., WEI W., HU X., and SUN D. A degradation phase division technique based on Gath–Geva fuzzy clustering. *JVC/Journal Vib. Control*, 2020, 26(15–16): 1147–1154. https://doi.org/ 10.1177/1077546319895110

[29] HU X., LI Y., JIA L., and QIU M. A novel two-stage unsupervised fault recognition framework combining feature extraction and fuzzy clustering for collaborative AIoT. *IEEE Transactions on Industrial Informatics*, 2021: 1–10. https://doi.org/ 10.1109/TII.2021.3076077

[30] GANESAN R., DAS T. K., SIKDER A. K., and KUMAR A. Wavelet-based identification of delamination defect in CMP (Cu-low k) using nonstationary acoustic emission signal. *IEEE Transactions on Semiconductor*

Manufacturing, 2003, 16(4): 677–685. https://doi.org/ 10.1109/TSM.2003.818975
[31] LI J., HAN Z., LUO H., CAO J., and ZHANG Y. Investigations of the fatigue damage in 16Mn steels by wavelet-based acoustic emission technique. In: *Proceedings of the IEEE 2012 Prognostics and System Health Management Conference (PHM-2012), Beijing, 23-25 May 2012*. Piscataway, New Jersey: Institute of Electrical and Electronics Engineers, 2012: 1-5.
https://doi.org/ 10.1109/PHM.2012.6228805
[32] MERRY R. *Wavelet theory and applications. A literature study*. Eindhoven: Technische Universiteit Eindhoven, 2005.
[33] JAIN A. K. and DUBES R. C. *Algorithms for clustering data*. Englewood Cliffs, New Jersey: Prentice-Hall, 1988.

参考文:

[1] HREN M.、BOSILJKOV B. V. 和 LEGAT A. 混合水泥和碳化對氯化物引起的腐蝕傳播的影響。水泥與混凝土研究，2021，145：106458。https://doi.org/10.1016/j.cemconres.2021.106458
[2] MANGALGIRI P. D. 飛機結構健康監測中的腐蝕問題。ISSS 微型與智能係統雜誌，2019 ，8(1): 49–78。https://doi.org/10.1007/s41683-019-00035-z
[3] KARVELIS P.、GEORGOULAS G.、KAPPATOS V. 和 STYLIOS C. 使用聲發射方法對船體進行結構健康監測的深度機器學習。船舶和海上結構，2020，16(1)：1-9。https://doi.org/10.1080/17445302.2020.1735844
[4] GOLDARAN R.、TURER A. 和 OZLUTAS K. 利用聲發射技術識別預應力混凝土管道中的腐蝕。建築與建築材料, 2020, 242: 118053. https://doi.org/10.1016/j.conbuildmat.2020.118053
[5] CALABRESE L.、GALEANO M.、PROVERBIO E.、DI PIETRO D.、CAPPUCCINI F. 和 DONATO A. 通過聲發射技術監測氯化物溶液中含硫代硫酸鹽的13%鉻馬氏體不銹鋼腐蝕。腐蝕科學，2016，111：151-161。https://doi.org/10.1016/j.corsci.2016.05.010
[6] MORIZET N.、GODIN N.、TANG J.、MAILLET E.、FREGONESE M. 和 NORMAND B. 使用小波和隨機森林對聲發射信號進行分類：在局部腐蝕中的應用。機械系統和信號處理，2016 ，70-71：1026-1037。https://doi.org/ 10.1016/j.ymssp.2015.09.025
[7] WU K.、ITO K.、SHINOZAKI I.、CIVAVIBUL P. 和 ENOKI M. 使用聲發射和 X 射線計算機斷層掃描對13鉻馬氏體不銹鋼局部腐蝕和應力腐蝕開裂的比較研究。材料（巴塞爾），2019 年，12(16): 1-19。https://doi.org/10.3390/ma12162569
[8] 張震, 吳新., 譚俊. 聲發射波形分析304不銹鋼高溫水中應力腐蝕開裂的原位監測.腐蝕科學，2019，146：90-98。https://doi.org/10.1016/j.corsci.2018.10.022
[9] CALABRESE L.、CAMPANELLA G. 和 PROVERBIO E. 在預應力混凝土樑的長期聲發射監測期間通過單變量和多變量統計分析識別腐蝕機制。腐蝕科學，2013，73：161-171。 https://doi.org/10.1016/j.corsci.2013.03.032
[10] ZIEHL M., MATTA F., VELEZ W. 預應力混凝土椿早期腐蝕的聲發射監測。結構控制和健康監測，2014，22(5)：873–887。https://doi.org/10.1002/stc.1723
[11] ABOUHUSSIEN A. A. 和 HASSAN A. A. A. 大型鋼筋混凝土梁腐蝕損傷傳播的聲發射監測。建築設施性能雜誌，32（2）：04017133。https://doi.org/ 10.1061/(ASCE)CF.1943-5509.0001127
[12] DAS A. K.、SUTHAR D. 和 LEUNG C. K. Y.. 基於未標記聲發射波形特徵的基於機器學習的裂紋模式分類。分和具体研究, 2019, 121: 42-57。https://doi.org/10.1016/j.cemconres.2019.03.001
[13] HESSER D. F.、MOSTAFAVI S.、KOCUR G. K. 和 MARKERT B. 基於卷積神經網絡和深度遷移學習的結構健康監測應用聲發射源的神經計算識別。神經計算，2021 ，453：1-12。https://doi.org/10.1016/j.neucom.2021.04.108
[14] SHEIKH M. F.、KAMAL K.、RAFIQUE F.、SABIR S.、ZAHEER H. 和 KHAN K. 使用基於聲發射和機器學習的方法進行腐蝕檢測和嚴重程度預測。艾因·沙姆斯工程雜誌，2021年5月，印刷中。https://doi.org/10.1016/j.asej.2021.03.024
[15] PAPPAS Y. Z.、MARKOPOULOS Y. P. 和 KOSTOPOULOS V. 使用聲發射監測對二維碳/碳進行失效機制分析。英美煙草國際，1998，31(3)：157–163。https://doi.org/10.1016/S0963-8695(98)00002-4
[16] SHAHIDAN S.、PULLIN R.、HOLFORD K. M.、MUHAMAD B. N. 和 NOR N. 混凝土梁中拉伸裂縫和剪切運動之間關係的定量評估。先進材料研究，2013，626：355-359。https://doi.org/10.4028/www.scientific.net/AMR.626.355
[17] JOHNSON M. 使用主成分分析對複合層壓板中的 AE 瞬變進行基於波形的聚類和分類英美煙草國際, 2002, 35(6): 367–376。https://doi.org/10.1016/S0963-8695(02)00004-X
[18] GAERTNER S. H. R., GODIN N. 整合科霍宁自組織圖和克均值算法，用於對交叉層複合材料拉伸測試期間收集的AE數據進行分割。无损检测國際, 2005, 38(4): 299–309。https://doi.org/ 10.1016/j.ndteint.2004.09.006
[19] BAR H. N.、BHAT M. R. 和 MURTHY C. R. L. 使用聚偏氟乙烯傳感器識別玻璃钢中的故障模式：人工神经网络方法。複合結構，2004，65（2）：231-237。https://doi.org/10.1016/j.compstruct.2003.10.019
[20] MARQUES A. T., DE OLIVEIRA R. 使用聲學电磁干扰對玻璃钢進行健康監測连接和人工神經

網絡。計算機與結構，2007，86（3）：367–373。https://doi.org/10.1016/j.compstruc.2007.02.015
[21] PHILIPPIDIS T.P.、NIKOLAIDIS V.N.、ANASTASSOPOULOS A. 使用神經網絡技術對 AE 信號進行碳/碳層壓板的損傷表徵。英美煙草國際， 1998, 31(5): 329–340。https://doi.org/10.1016/S0963-8695(98)00015-2
[22] HUGUET S.、GODIN N.、GAERTNER R.、SALMON L. 和 VILLARD D. 使用聲發射來識別玻璃纖維增強聚酯中的損傷模式。複合材料科學與技術，2002，62(10-11)：1433-1444。https://doi.org/ 10.1016/S0266-3538(02)00087-8
[23] BHAT C.、BHAT M. R. 和 MURTHY C. R. L. 使用人工神经网络的複合材料失效模式的聲發射特性。複合結構，2003，61(3)：213-220。https://doi.org/ 10.1016/S0263-8223(03)00068-0
[24] OMKAR S.N., RAGHAVENDRA KARANTH U. 使用蟻群優化對聲發射信號進行分類的規則提取。人工智能的工程應用， 2008, 21(8): 1381-1388. https://doi.org/10.1016/j.engappai.2008.02.004
[25] BEHNIA A.、CHAI H. K.、GHASEMIGOL M.、SEPEHRINEZHAD A. 和 MOUSA A. A. 通過將無監督聚類集成到聲發射中的高級損傷檢測技術。工程斷裂力學，2019，210：212-227。https://doi.org/10.1016/j.engframech.2018.07.005
[26] EBRAHIMKHANLOU A. 和 SALAMONE S. 使用深度學習的板狀結構中的單傳感器聲發射源定位。航空航天，2018，5(2)：1-22。https://doi.org/10.3390/aerospace5020050。
[27] SUWANSIN W. 和 PHASUKKIT P. 基於深度學習的聲發射方案，用於在負載下無損定位火車軌道裂紋。傳感器（瑞士），2021，21(1): 1-19。https://doi.org/ 10.3390/s21010272
[28] WANG B., WEI W., HU X., 和 SUN D. 基於加特-吉瓦模糊聚類的退化階段劃分技術。合资公司/日记本。控制，2020，26（15-16）：1147-1154。https://doi.org/10.1177/1077546319895110
[29] HU X., LI Y., JIA L. 和 QIU M. 一種新的兩階段無監督故障識別框架，結合特徵提取和模糊聚類，用於協同物联网。IEEE工業信息學彙刊，2021：1-10。https://doi.org/10.1109/TII.2021.3076077
[30] GANESAN R.、DAS T. K.、SIKDER A. K. 和 KUMAR A. 使用非平穩聲發射信號對 CMP（铜-低克）中的分層缺陷進行基於小波的識別。IEEE半導體製造彙刊，2003，16(4)：677–685。https://doi.org/10.1109/TSM.2003.818975
[31] LI J., HAN Z., LUO H., CAO J., 和 ZHANG Y. 基於小波聲發射技術的 16锰鋼疲勞損傷研究。在：IEEE 2012年預測和系統健康管理會議(PHM-2012)的論文集，北京，2012年5月23-25日。新澤西州皮斯卡塔韋：電氣和電子工程師協會，2012 ：1-5。https://doi.org/10.1109/PHM.2012.6228805
[32] MERRY R. 小波理論與應用。文學研究。埃因霍溫：埃因霍溫工業大學，2005。
[33] JAIN A. K. 和 DUBES R. C. 數據聚類算法。新澤西州恩格爾伍德懸崖：普倫蒂斯霍爾，1988.